Chapter 6

Increasing the membrane fusion efficiency by reducing undesired peptide-peptide interactions

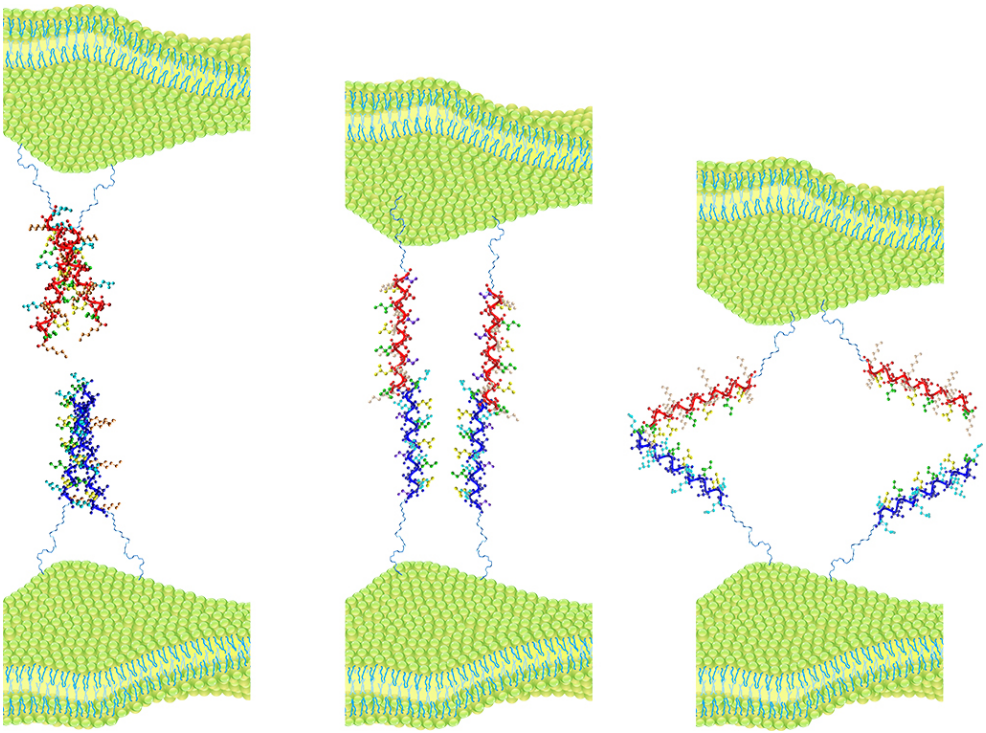

Zheng, T. T.; Boyle, A.; Marsden, H. R.; Kros, A., Raising membrane fusion efficiency by reducing fusogen homo interaction. Manuscript in preparation.

Abstract

The effect of Coil-K peptide homo interaction on coiled coil CC-K/E mediated liposome fusion efficiency was investigated. Coil-K clustering on liposome membranes was tuned by changing the electrostatic interaction between peptides. For this, the original amino acid sequence of Coil-K was varied at the f-position. The glutamate residue ('E') was replaced with either a serine ('S', no charge) or a lysine ('K', positive charge) residue, yielding Coil-K_S and Coil-K_K. Circular dichroism (CD) and fluorescence spectroscopy confirmed that the peptide modifications did not influence the coiled coil formation with the complementary peptide Coil-E. CD studies of lipidated Coil-K_S and Coil-K_K incorporated in liposomal membranes revealed that more electrostatic repulsion between the peptides increased the fusogenity. Lipid and content mixing assays showed more efficient liposome-liposome fusion using Coil-K_k and Coil-K_s in conjunction with coil-E. A probable cause for this effect might be that repulsion between the peptides in the pre-fusion state results in a more homogeneous peptide distribution on the liposomal membrane.

Introduction

The 2013 Nobel Prize in Physiology or Medicine was awarded to James Rothman, Randy Schekman and Thomas Südhof for their seminal contributions in understanding vesicular transport mechanisms in cells.[1] One of the important actors in membrane trafficking, so called SNARE proteins (soluble N-ethyl maleimide sensitive factor attachment protein receptors), mediate membrane fusion and are widely studied.[2-4] In nature, the distance between biological membranes is typically around 10- 20 nm, due to the electrostatic repulsion between the charged bilayers and the steric interaction of membrane bound proteins and other biomolecules.[5] Thus the first step of a fusion event is to bring the opposing membrane lipid bilayers into close proximity. Next, local disruption of the bilayer structure results in the formation of a stalk-like structure (Scheme 1). In the stalk intermediate the outer membranes of the approaching lipid bilayers have merged, but not the inner leaflets. It is believed that the stalk which expands into a hemifusion stalk or diaphragm, subsequently enlarges such a pore is being formed. As a result, the contents of the compartments mix, and the fusion process is completed.[6, 7]

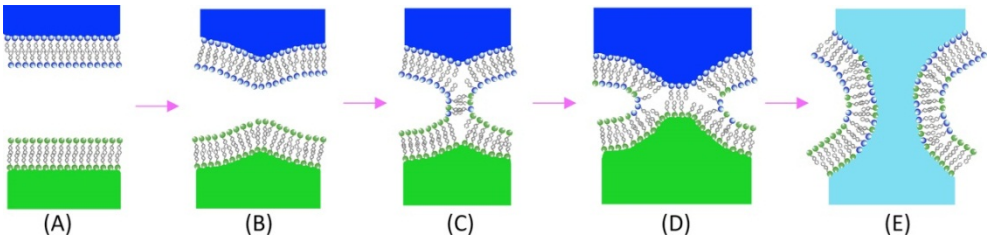

Scheme 1. (A) Two opposing membranes in the pre-fusion state. (B) A point-like membrane protrusion minimizes the energy of the hydration repulsion between the proximal leaflets of the membranes coming into immediate contact. (C) A hemifusion stalk with proximal leaflets fused and distal leaflets fused and distal leaflets unfused. (D) Stalk expansion yields the hemifusion diaphragm. (E) A fusion pore forms either in the hemifusion diaphragm bilayer or directly from the stalk (take from reference 5).[8]

The lipid rearrangements of membrane fusion during intracellular transport are mediated by SNARE proteins.[4] However, the molecular mechanism is still debated. To induce membrane fusion, a four-helix coiled-coil bundle forms between two membrane-bound SNARE protein subunits and a cytoplasmic SNARE protein subunits forcing the two membranes within a distance of 2-3 nm from one another, resulting in docking of the two opposing membranes followed by lipid and content mixing.[5, 9] Inspired by this natural and highly controlled transport mechanism, supramolecular and biomaterials chemists designed synthetic targeted membrane fusion systems to study the mechanism of membrane fusion at a fundamental level, or to explore future applications in drug delivery or in the design of nanoreactors. Our previously published synthetic membrane fusion system has shown to be very effective in inducing liposome-liposome fusion (Scheme 2).[10-12] There are three key components in the design of our fusion model. First there is the molecular recognition part, which drives the membrane of two liposomes into close proximity. For this we use the complementary peptides Coil-K and Coil-E, which were designed to form a heterodimeric coiled coil complex.[10, 13] Flexibility and rotational freedom of the peptides is ensured by conjugation of a poly(ethylene glycol) spacer (PEG_{12}) at the N-terminus of the peptides. The third component in our design is the lipid anchor 1,2-dioleoyl-*sn*-glycero-3-phosphoethanolamine (DOPE), which is conjugated to the PEG spacer. This guarantees that the peptides will anchor into a lipid bilayer (Scheme 2).

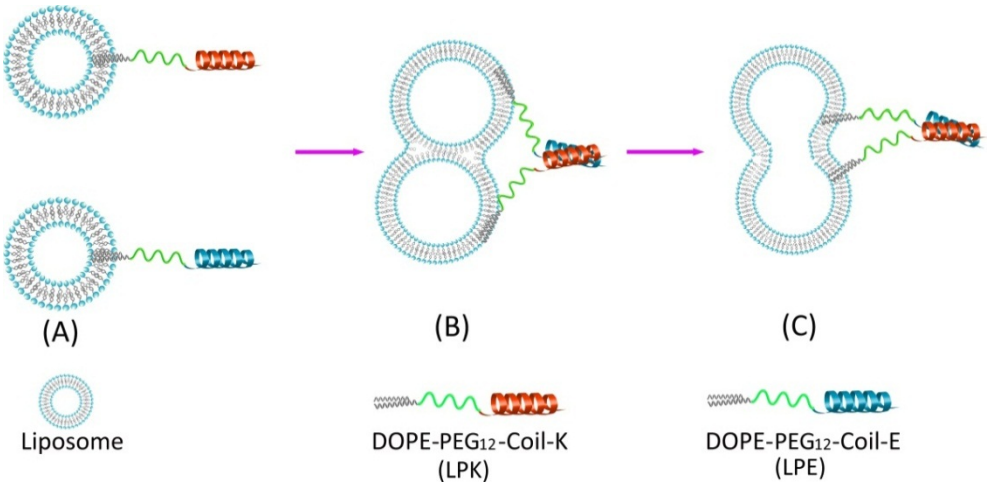

Scheme 2. Illustration of liposome fusion mediated by lipopeptides, as well as an overview of the lipopeptides used in this study. Liposomes are decorated with LPK (red) or LPE (blue) and upon mixing coiled-coil formation brings the opposite liposomes in close proximity, and ultimately leads to fusion.

From previous experiments, we realized that peptide homo-aggregation on the liposomal membrane before fusion reduces its fusion efficiency with the complementary fusion partner.[11] It seems that there is an optimal peptide to lipid ratio of ~0.75 mol%. Higher ratios did not result in faster fusion. Circular dichroism (CD) spectroscopy showed that at high fusogen concentrations on the membrane, self-aggregation due to homocoiling and increased peptide-membrane interactions seem to occur resulting in a heterogeneous distribution of the peptides on the liposome surface.

A driving force for the observed peptide aggregation might be electrostatic interactions. In the original coiled coil (CC) K/E design, position ‘a’ and ‘d’ in the helical wheel diagram are taken by the amino acid residues isoleucine (I) and leucine (L) respectively, forming the hydrophobic core (Scheme 3). Position ‘b’ and ‘c’ are occupied by alanine (A), which increases the propensity of the peptide to adopt an α-helical configuration.[14] Heterodimerization was programmed by incorporating charged residues at position ‘e’ and ‘g’, adjacent to the hydrophobic core, being lysine (K) residues in peptide Coil-K and glutamate residues (E) in the Coil-E peptide. This coiled coil was designed to function at neutral pH, where the side chains of all lysine residues are protonated, and hence positive charged, while the side chains of all glutamate residue residues are deprotonated and hence negatively charged. The final position in the heptad repeat, position ‘f’, was occupied by an

opposite charge relative to positions ‘e’ and ‘g’, in order to decrease the overall net charge of the single peptide. Due to the existence of opposite charges residues within one single peptide, electrostatic attraction could cause undesired peptide-peptide interactions at the membrane of the liposomes. This in turn lowers the effective monomeric peptide concentration at the membrane, resulting in the observed lower fusogenity at higher peptide concentrations. Circular dichroism and dynamic light scattering data shows that the acetylated peptides (i.e. no lipid anchor) uniformly disperse in PBS buffer (pH=7.4), with no noticeable homo-interaction being observed. However, the situation changes when the peptides are confined on a liposome surface. When the peptides are fixed to a liposomal surface through the phospholipid anchor, Coil-K peptide shows significantly homo-interaction and peptide-membrane interactions, as observed in CD measurements.[11] However, it is important to note that this does not result in fusion. By decreasing the Coil-K density on liposome surface to 0.75 mol%, the peptide self-interaction significantly decreased and coincidentally, the liposome fusion lipid mixing rate increased.

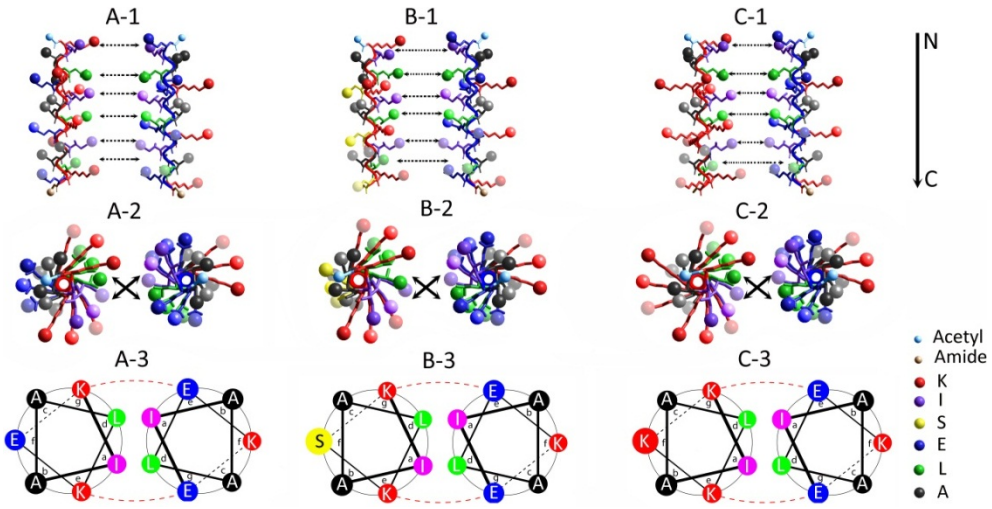

Scheme 3. Parallel heterodimeric peptide used in this study. (A) column shows Coil-K (left) with Coil-E (right), (B) column shows Coil-K_S (left) with Coil-E (right), and (C) column shows Coil-K_K (left) with Coil-E (right). (A-1) presents lateral view of CC-K/E, (A-2) presents top view of CC-K/E (from N to C- terminus), (A-3) presents simplified top view (from N to C- terminus), so-called helical wheel of CC-K/E (same with column (B) and (C)). Amino acid were expressed by signal letter (K= lysine, I= isoleucine, S= serine, E =glutamate, L= leucine, A= alanine). Black arrows indicate hydrogen bonding, while red imaginary lines indicate helical interface electrostatic attraction.

To investigate whether electrostatic interactions have an effect on Coil-K homo-interaction, the influence of a charge at position 'f' in peptide coil-K on the rate of membrane fusion was studied. Thus, the liposome fusion efficiency was investigated as a function of peptide aggregation by tuning the electrostatic interaction between the peptides on the liposomal surface (Scheme 4). Besides the original Coil-K with a glutamate residue at position 'f', two new sequences were synthesized with either the noncharged serine (S) or the positive charged lysine on position 'f', denoted Coil-K_S and Coil-K_K respectively. The aim here is to increase the electrostatic repulsion between the peptides, and thereby increasing the effective peptide concentration able to form a coiled coil motif with peptide Coil-E yielding a higher fusion efficiency.

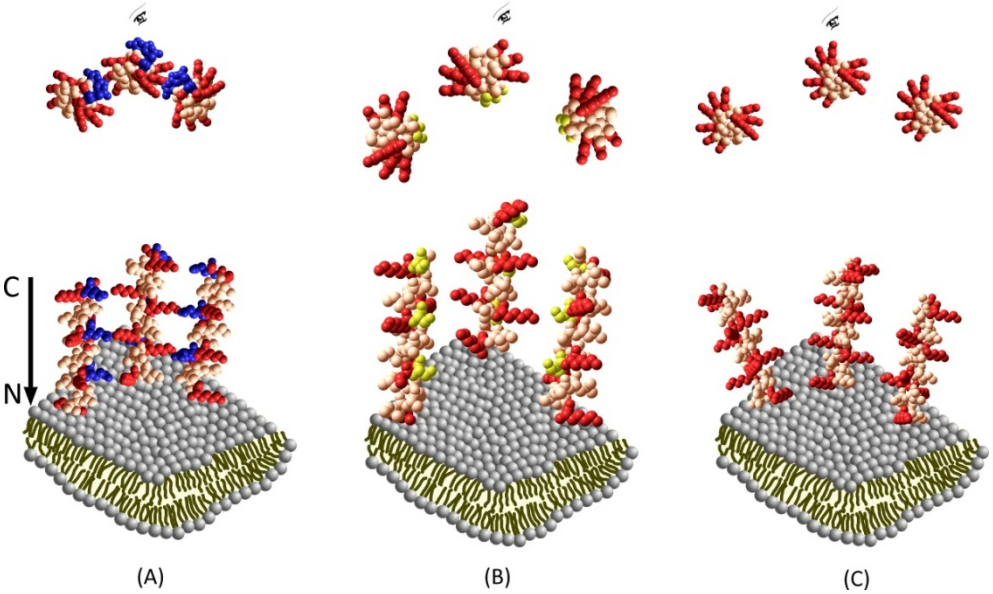

Scheme 4. Proposed peptide electrostatic interactions on liposome membrane surfaces (lower) and vertical view of peptides from C to N terminus (upper). (A) indicates interactions among Coil-K peptides when they are anchored on the membrane with crowded surface density. Identically, (B) indicates Coil-K_S interactions, while (C) indicates Coil-K_K interactions. Peptides were modeled by Hyperchem release 8.0 as classical L-alpha helix, with three dihedral angels: ϕ= -58^o, ψ= -47^o, ω=180^o. Amino acid residues were illustrated by using balls atom rendering. Positive charged lysine residues are in red, negative charged glutamate in blue and '0'net charged serine in yellow, meanwhile other zero net charged residues are in orange. Uniformly, gray bilayers indicates liposome membrane surfaces, PEG_{12} linker and DOPE anchor are omitted for clarity.

Circular Dichroism (CD) spectroscopy showed that replacing the glutamate residues at position 'f' with serine or lysine reduces their tendency to aggregate. Fluorescence resonance energy transfer (FRET) measurements revealed that less peptide aggregation on liposomal membranes resulted in an increased lipid mixing rate in membrane fusion studies. More importantly, content mixing assays based on fluorescence dequenching of rhodamine B showed a significant increase in fusion efficiency for the least aggregated peptide Coil-K_K. These findings indicate that an increase in electrostatic repulsion yields less interacting Coil-K_K in the pre-fusion state. Upon the addition of liposomes bearing the complementary peptide Coil-E, efficient fusion was observed for the least aggregated peptides. Thus, we successfully optimized our fusion model system resulting in a more efficient rate of content mixing.

Results and discussion

Peptide interaction study

Peptide design

In this study, the charged amino acid residue at 'f' position has been varied, yielding new coil-K peptide mutants, as shown in Table 1.[11, 15]

Table 1. peptide primary structure

Name	Sequence and residue charge	Molecular Weight (theoretical) ($g \cdot mol^{-1}$)	Molecular Weight (experimental) ($g \cdot mol^{-1}$)
Coil-K	Ac-(KIAALKE)$_3$-CONH$_2$ (+ + −)	2320.89	2320.40
Coil-K_S	Ac-(KIAALKS)$_3$-CONH$_2$ (+ +)	2194.78	2194.41
Coil-K_K	Ac-(KIAALKK)$_3$-CONH$_2$ (+ + +)	2318.07	2317.59
Coil-E	Ac-(EIAALEK)$_3$-CONH$_2$ (− − +)	2323.71	2323.34

'+' stands for positive charge, '-'stands for negative charge. Yellow column indicates the 'f' position. Sequence presents from N terminus to C terminus. All peptides were acetylated.

Instead of the negatively charged glutamate residue, we introduced either the non-charged serine (S) or the positively charged lysine (K), yielding two new peptides Coil-K_S and Coil-K_K respectively (Scheme 3). Furthermore, Coil-K (and its derivatives) and Coil-E were conjugated to DOPE via the flexible spacer PEG_{12} at the N-terminus for the fusion studies. This design ensures the binding of these lipidated peptides in the membranes of liposomes (vide infra).

Circular Dichroism Spectroscopy.

CD measurements showed that all the peptides adopt to some degree an α-helical structure in PBS buffer with the molar ellipiticity ratio $[\theta]_{222}/ [\theta]_{208} < 1$. However Coil-$K_S$ revealed a relatively low α-helicity (24 %) compared to coil-K and coil-K_K due to serine's poor propensity to adopt an α-helical conformation (Figure 1A and Table 2).[16] Next, the molar ellipticity of acetylated peptides was measured in a 1:1 (v/v%) mixture of trifluoroethanol (TFE) and PBS. TFE is known to enhance intramolecular α-helicity while disrupting intermolecular interactions.[17] The molar ellipticity, as measured at 222 nm, revealed an increase for all acetylated peptides in the presence of 50 % TFE, verifying their propensity to adopt an α-helical secondary structure and that no peptide aggregation was present in PBS.

When mixing equimolar amounts of Coil-K (or its derivatives: Coil-K_S, Coil-K_K) with Coil-E, the molar ellipticity intensity at 222 nm increased significantly (Figure 1C).[14] For all the peptide pairs, the ellipticity ratio $[\theta]_{222}/ [\theta]_{208}$, increased to > 1 (Table 2), which indicated the formation of coiled coils.[18] The peptide interactions were further studied by recording CD spectra in a 1:1 (v/v%) mixture of trifluoroethanol (TFE) and PBS. In this solvent mixture, the observed decrease in molar ellipticity and $[\theta]_{222}/ [\theta]_{208}$ ratios strongly suggest the presence of coiled coils, which are destabilized in the presence of TFE (Figure 1D). These initial results confirm that individual Coil-K (and its derivatives) and Coil-E peptides adopt a random coil to α-helical structure in PBS buffer. However, when Coil-K (Coil-K_S or Coil-K_K) are mixed with equimolar amounts of Coil-E, coiled coils are formed immediately. More importantly, this study showed that the charge at the 'f' position of coil-K peptides can be varied without compromising their ability to form coiled coils with coil-E.

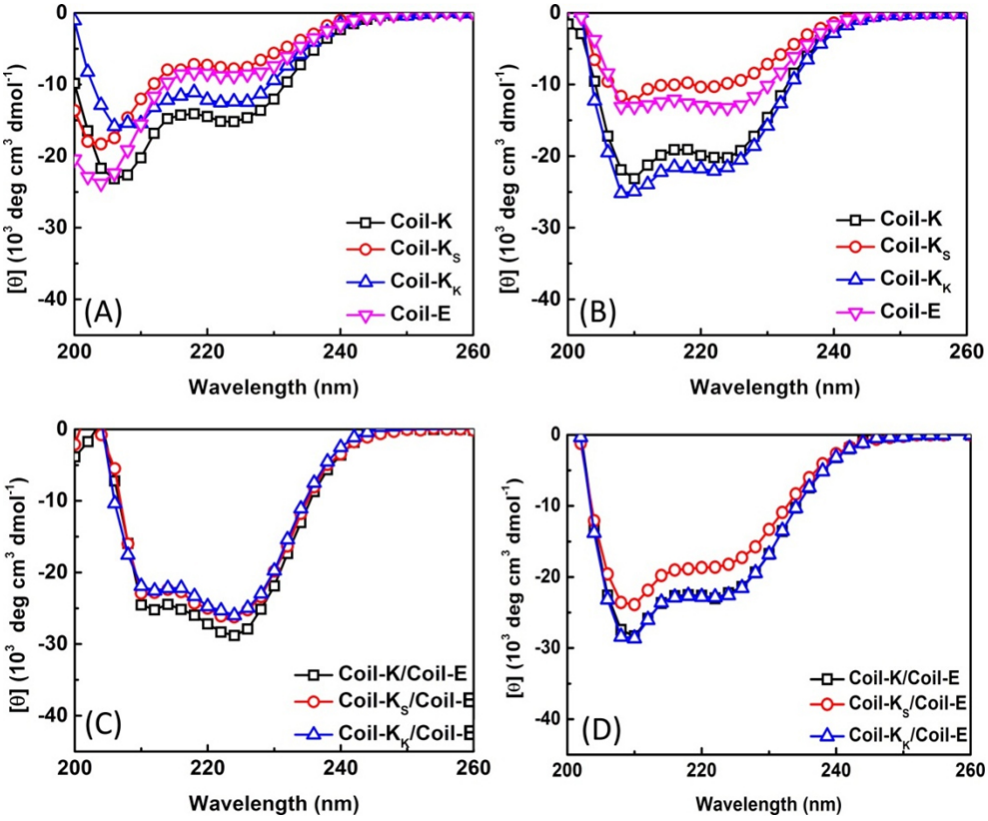

Figure 1. (A) CD spectra of the peptides in PBS buffer and (B) in 1:1 (v/v) PBS: TFE. (C) CD spectra of an equimolar mixture of the Coil-K variants and Coil-E in PBS buffer and (D) in 1:1 (v/v) PBS: TFE. [Total peptide]= 100 uM, pH 7.4, 25 °C.

Table 2. CD spectroscopic data of the acetylated peptides.

Name	$[\theta]_{222}$		$[\theta]_{208}$		$[\theta]_{222}/[\theta]_{208}$		%α-helix[a]	
	PBS	50% TFE	PBS	50% TFE	PBS	50% TFE	PBS	50% TFE
Coil-K	-15172	-20201	-22647	-21909	0.67	0.92	49	65
Coil-K_S	-7583	-10286	-14656	-11640	0.52	0.88	24	33
Coil-K_K	-12526	-22070	-15375	-25174	0.81	0.88	40	70
Coil-E	-8824	-13147	-19146	-13090	0.46	1.00	28	42

[a] The percentage α-helicity is the ratio of the observed $[\theta]_{222}$ to the predicted $[\theta]_{222}$ for an α-helical peptide of n residues times 100. The predicted α-helicity is calculated from $[\theta]_{222}$=-40000*(1-4.6/n).[18] (PBS buffer pH=7.4)

Table 3. CD spectroscopic data of the peptide complexes.

Complex[a]	$[\theta]_{222}$		$[\theta]_{208}$		$[\theta]_{222}/[\theta]_{208}$		%α-helix		Coiled-coil[b]
	PBS	50% TFE	PBS	50% TFE	PBS	50% TFE	PBS	50% TFE	
CC-K/E	-28323	-23016	-15946	-27449	1.14	0.84	91	74	+
CC-K_S/E	-26106	-18619	-16001	-23583	1.14	0.79	84	60	+
CC-K_K/E	-25314	-22833	-17551	-28388	1.15	0.84	81	73	+

[a] A/B refers to mixtures of the stated compounds with equimolar concentrations. [b] The + sign signifies a significant decrease in the $[\theta]_{222}/[\theta]_{208}$ ratio from benign to 50% TFE in PBS, indicative of the folded coiled-coil structure in PBS.

Next, the binding properties were determined of the coiled coil complexes (CC-K/E, CC-K_S/E, CC-K_K/E) by CD spectroscopy. A job-plot showing the $[\theta]_{222}$ as a function of the mol fraction of Coil-E peptide yields information on the binding stoichiometry of the coiled coils.[19, 20] The job-plot of Coil-K (and its derivatives) and Coil-E mixtures were measured with a total peptide concentration of 200 uM and with variable mol fractions of the two peptides. For all CC-K/E (including derivatives) coiled coil complexes studied, a minimum of $[\theta]_{222}$ was always observed at an equimolar ratio of peptide Coil-K (and derivatives) and Coil-E, revealing the formation of a coiled coil complex with a 1:1 stoichiometry (Figure 2A).

As the molar ellipticity at 222 nm is directly proportional to the amount of helical structure and therefore thermal denaturation curves provide information of their folding stabilities.[18, 21] Thus the thermodynamic stability of the CC-K/E pairs was determined by measuring the molar ellipticity at 222 nm wavelength as a function of temperature.[13, 22] All coiled coil pairs showed a smooth cooperative transition from a α-helical coiled coil structure to a random coil conformation (Figure 2B). All transitions showed to be fully reversible by lowering the temperature (See Appendix Figure A4). Temperature-dependent CD measurements showed that all the peptide complexes used in this study have an identical two-state transition denaturation process, dissociating from a coiled coil to random coils.

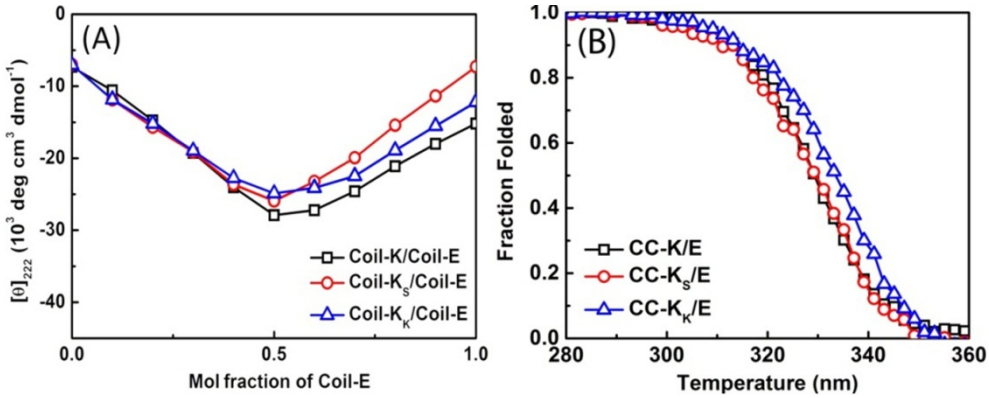

Figure 2. (A) Mean residue molar ellipticities at 222nm wavelength for mixtures of the Coil-K (or its derivants) and Coil-E peptides as a function of the mol fraction of the Coil-E peptide. [Total peptide]=100 uM, 25 ^{o}C, 2 mm quartz cuvette. (B) Thermal unfolding curves of coiled coils in PBS buffer (pH=7.4) with increasing temperature. A 1cm quartz cuvette with stirring bar at 900 rpm was used. [Total peptide]=40 uM, PBS, pH=7.4.

The binding parameters of the studied coiled coil heterodimers are summarized in Table 4. Either the similarity in binding stoichiometry or the resemblance in dissociation constant of all coiled coils show that replacing a glutamate (charge '-') with a serine (charge '0') or a lysine (charge '+') residue on the 'f' position in peptide Coil-K did not influence the ability to form coiled coils, while the changes in ΔG were minor.

Table 4. Binding constants of coiled coils from CD spectroscopy.

Peptide pair	T_m (°C) [b]	Stoichiometry	ΔG_u (kcal mol^{-1}) [c]	K_d (*10^{-8} M) [d]
CC-K/E [a]	56	1:1	10	6.7
CC-K$_S$/E	56	1:1	9.5	7.4
CC-K$_K$/E	60	1:1	9.9	5.4

[a] CC indicates coiled coil. [b] T_m=melting temperature, at which half of the peptide is in the unfolded form. c ΔG_u= Gibbs free energy of unfolding at 25 ^{o}C. [d] K_d=dissociation constant at 25 ^{o}C.

Fluorescence spectroscopy

The relative peptide orientation within a coiled coil motif (i.e. parallel vs antiparallel) was investigated by fluorescence spectroscopy. For this, Coil-K (Coil-K$_S$ and Coil-K$_K$) were labeled with a tryptophan (W) at the C-terminus, yielding Coil-K' (Coil-K$_S$' or Coil-K$_K$',

see Table 5). In addition, Tyrosine (Y) was added to the C-terminus of Coil-E, giving Coil-E'. As mentioned in Chapter 3 and Chapter 4, glycine (G) was added in between aromatic amino acid (W and Y) and original peptide sequence to avoid significant structure alteration. The relative orientation of the two peptides within a coiled coil complex was confirmed by a fluorescence resonance energy transfer (FRET) between the donor Y on Coil-E', and the acceptor W on Coil-K' (including its derivatives). Both fluorophores are at the C-termini of the peptides, and the Förster distance ($R_0 \approx$ 1 nm) is shorter than the length of the peptides in a α-helical fashion (~ 3-4 nm) (see Appendix, Figure A4), which stringently ensures that FRET can only occur when the peptides are assembled with a parallel orientation, not when an antiparallel orientation is adopted.[23]

Table 5. Fluorescent labeled peptide primary structure

Name	Sequence and residue charge [a]	Mw ($g \cdot mol^{-1}$) [b] (theoretical)	Mw ($g \cdot mol^{-1}$) (experimental)
Coil-K'	Ac-$(KIAALKE)_3$-GW-$CONH_2$	2563.6	2564.15
Coil-K_S'	Ac-$(KIAALKS)_3$-GW-$CONH_2$	2437.59	2438.04
Coil-K_K'	Ac-$(KIAALKK)_3$-GW-$CONH_2$	2560.59	2561.33
Coil-E'	Ac-$(EIAALEK)_3$-GY-$CONH_2$	2543.61	2543.94

[a] All the peptides primary structures present from N to C terminus. [b] Mw= molecular weight.

Figure 3 shows the emission spectra (excitation at 275 nm) of peptides Coil-K' (and its derivatives) and Coil-E', CC-K'/E' (including its derivatives) in PBS and in 1:1 PBS: TFE solution. An equimolar mixture of Coil-K' and Coil-E' results in an increased fluorescence signal of acceptor W and a decreased fluorescence signal of donor Y due to fluorescence resonance energy transfer (FRET), thus indicating a parallel coiled coil orientation for CC-K'/E' (Figure 3A). In the presence of 50% TFE, the energy transfer is lost due to the dissociation of coiled coil complex. Consistently, CC-K_S'/E and CC-K_K'/E also showed a parallel coiled coil orientation (Figure 3B, C).

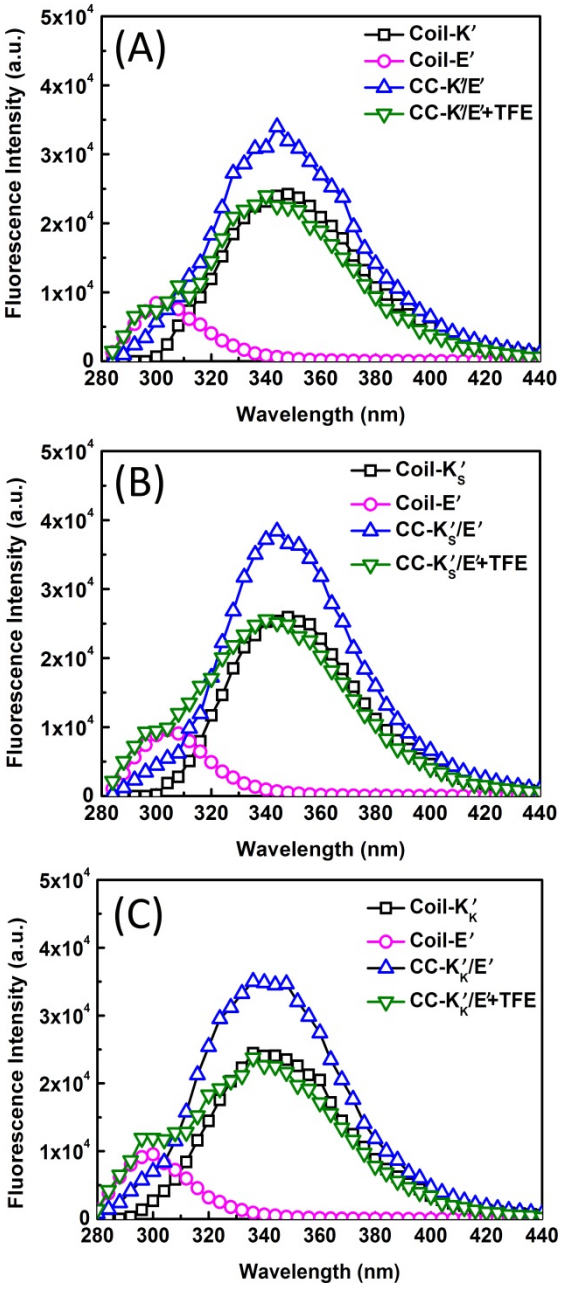

Figure 3. Fluorescence emission spectra (extension at 275 nm) of fluorescent labeled peptides 50 uM in either pH=7.4 PBS buffer or 1:1 TFE/PBS solution on 25 ^{o}C. (A) Coil-K'=Ac-$(KIAALKE)_3$-GW-$CONH_2$, Coil-E'=Ac-$(EIAALEK)_3$-GY-$CONH_2$. (B) Coil-

K_S'=Ac-(KIAALKS)$_3$-CONH$_2$. (C) Coil-K_K'=Ac-(KIAALKK)$_3$-CONH$_2$. W is tryptophan, while Y is tyrosine.

Both CD and fluorescence measurements showed that replacing the negatively charged glutamate residue at the 'f' position with either the positively charged lysine or non-charged serine on position 'f' in Coil-K did not significantly alter the peptide ability to form a coiled coil. Hence, we consider the electrostatic interaction as the only difference in the following liposome fusion studies.

Lipopeptide mediated liposome fusion study

Lipopeptide synthesis

The lipopeptides were synthesized as previously mentioned in Chapter 5. However, the lipopeptides cleavage from the resin was optimized by using a cocktail of TFA, DCM, phenol and TIS (70:22.5:5:2.5% v/v) for peptide precipitation. The purification of the crude lipopeptides was performed as described in Chapter 5 and the resulting products are presented in Table 6.

Table 6. Lipopeptides used in this study

Name	Mw (g·mol^{-1}) [a] (theoretical)	Mw (g·mol^{-1}) (experimental)	Yield [b]	Purity [c]
LPK	3704.10	3704.01	60 %	>95 %
LPK_S	3577.88	3577.80	65 %	>95 %
LPK_K	3701.00	3701.19	50 %	>95 %
LPE	3706.82	3706.54	63 %	>95 %

a Mw is molecular weight. b and c were calculated after HPLC purification.

CD spectroscopy

The peptides were incorporated into the surface of liposomal membranes at a concentration of 1 mol%. Compared with the acetylated peptides in PBS, the membrane bound lipopeptides showed a red shift in the minumum (from 222 nm to 225 nm) in the CD

spectra (Figure 4). This is due to different dielectric of the membrane environment relative to that of single peptides in aqueous buffered solutions.[24-26]

CD measurements of lipopeptide LPK in liposomes revealed a $[\theta]_{225}/[\theta]_{208}$ ratio larger than 1, indicating that it has a tendency to either homocoil or interact with the lipid membrane (Figure 4A). In contrast, the other individual lipopeptides (LPK_S, LPK_K and LPE) all showed a $[\theta]_{225}/[\theta]_{208}$ ratio <1, implying that homocoiling occurring at the membrane was significantly suppressed.[22, 27] Upon equimolar mixing of LPE-modified liposomes with LPK-modified liposome, immediate coiled coiling of the peptides was observed as well as peptide aggregation since the ellipticity ratio increased significantly to larger than 1 (Figure 4B).[28] This ellipticity ratio increase was less pronounced for mixtures of LPK_S (or LPK_K) liposomes interacting with LPE liposomes. This circular dichroism study indicates that changes of the charge at the 'f' position in coil-K influences the peptide behavior at the liposomal membrane, most likely by decreasing the tendency to self-aggregate in the prefusion state.

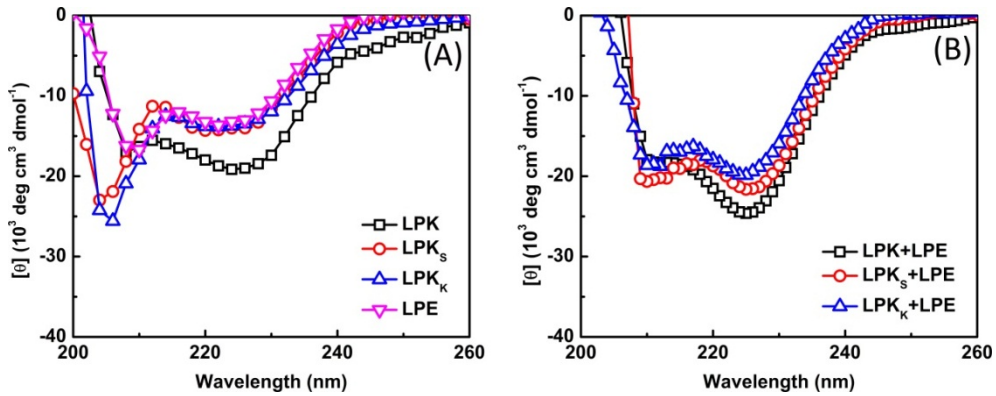

Figure 4. (A) Circular dichroism spectra of 1 mol% lipopeptide on liposomal membranes. (B) Equimolar mixture of LPK (and its derivatives) and LPE on liposomes. [Lipids]=0.5 mM, PBS buffer, pH=7.4, 25 ^{o}C.

Liposome fusion studies

The effect of charge at the 'f' position of coil-K on the rate of membrane fusion was studied with lipid and content mixing assays as well as dynamic light scattering (DLS). In general, the process of liposome fusion is initiated by docking of two opposing liposome membranes in close proximity, followed by the formation of a so-called the stalk

intermediate and merging of two liposomes outer lipid leaflets (Scheme 1). Finally, a membrane pore is formed resulting in content mixing between the two liposomes. Coiled coil formation between the two complementary peptides on the opposing membranes is the driving force inducing liposome docking followed by fusion. Peptide aggregation at the surface of liposomes in the pre-fusion state might lead to steric hindrance at the membrane and/or lowering the effective peptide concentration. As a result, fewer peptides are available to form coiled coils which lowers the liposome fusion rate and efficiency.[11, 28]

First, the rate of lipid mixing was determined by a standard FRET assay. Coil-K modified liposomes (shortname K-L_F), contained both the donor dye nitrobenzofuran (NBD) and the acceptor dye lissamine rhodamine (LR) attached to the membrane, while Coil-E modified liposomes (shortname E-L) were not decorated with fluorescent dyes. These liposomes were stable with time and did not show any self-aggregation or fusion for at least 24h (See Appendix Figure A6). Upon equimolar mixing of K-L_F liposomes with E-L liposomes, an immediate increase in the NBD emission was observed as a result of a decreased FRET efficiency due to the increase in the average distance between NBD and LR. This is due to lipid mixing between K-L_F and E-L liposomes. Figure 5A shows that in all three experiments full lipid mixing (i.e. 100%) was achieved within 60 min. However, fusion between K_K-L_F and E-L liposomes showed the highest initial lipid mixing rate. Also fusion between K_S-L_F with E-L liposomes resulted in a higher lipid mixing rate as compared to the fusion induced by the original coil-K and coil-E peptides. Thus, varying the charge in coil-K at the 'f' position resulted in differences in the initial lipid mixing rate, albeit these became smaller at longer time scales.

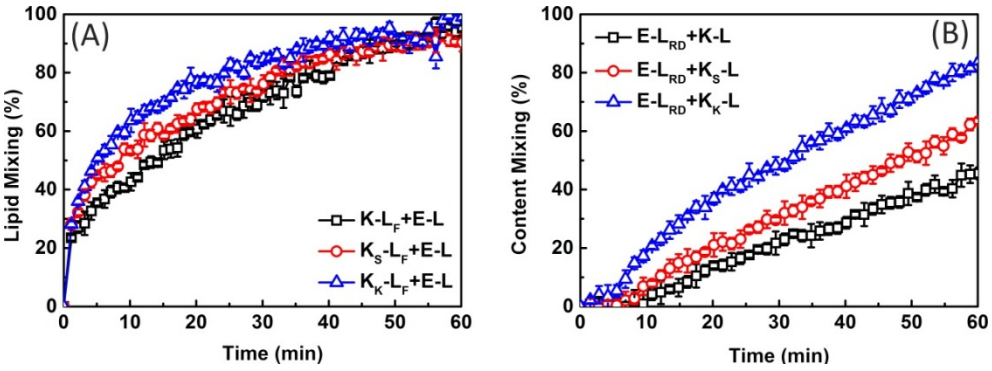

Figure 5. (A) Fluorescence traces showing lipid mixing between fluorescence (NBD/LR) labeled LPK (and derivatives) liposomes with non-fluorescence labeled LPE liposomes. (B)

Content mixing between non-fluorescent LPK liposomes with sulforhodamine labelled (20 mM) LPE liposomes. Liposome concentration is 0.1 mM with 1% peptide decoration. The bars show the standard deviations (σ). See Figure A6/A7 for the lipid mixing and content mixing fluorescence spectra. All the measurements were performed in PBS, pH 7.4, at 25 ^{o}C.

Next, a liposome fusion content mixing assay was performed, which revealed a more pronounced difference between the three pairs of lipidated peptides (i.e. CC-K/E, CC-K_S/ E, CC-K_K/E). In this experiment, Coil-E modified liposomes were loaded with sulphorhodamine B at a self-quenching concentration of 20 mM, yielding E-L_{RD} liposomes, while Coil-K (including its derivatives) modified liposome did not contain dyes in the aqueous interior, yielding K-L liposomes. Upon mixing of the liposomes, fusion resulted in the transfer of content transfer with a concomitant dilution of the rhodamine dye, thereby alleviating the self-quenching and a subsequent increase in fluorescence intensity (Figure 5B).

Here, significant differences in content mixing were observed as a function of the peptides used. Within 60 min, fusion between E-L_{RD} liposomes and K_K-L liposomes yielded 85% of content mixing, which is significantly higher as compared to the original peptide design (i.e. coil-K/coil-E modified liposomes) Using coil-K_S/coil-E modified liposomes with a neutral charge at the ‘f’ position also gave an increased fusion efficiency, but less pronounced when compared to the coil-K_k/coil-E liposomes.

Dynamic light scattering

To study the size increase due to aggregation and fusion events upon mixing of the liposomes, we used dynamic light scattering (DLS) measurements in order to determine whether the average liposome size increase correlated with the lipid and content mixing results. The results revealed similar initial docking rate and size increasing due to the limited instrumental sensitivity. It is important to note that dynamic light scattering cannot distinguish between liposome-liposome docking and liposome-liposome fusion events. Therefore it can be concluded that all studied coiled coil pairs were able to at least induce docking between opposing liposomes with comparable efficiency. After 30 minutes the increase in the hydrodynamic diameter deviates. However, at these diameters DLS becomes less reliable and therefore it is difficult to draw any conclusions on the size increase in this time range.

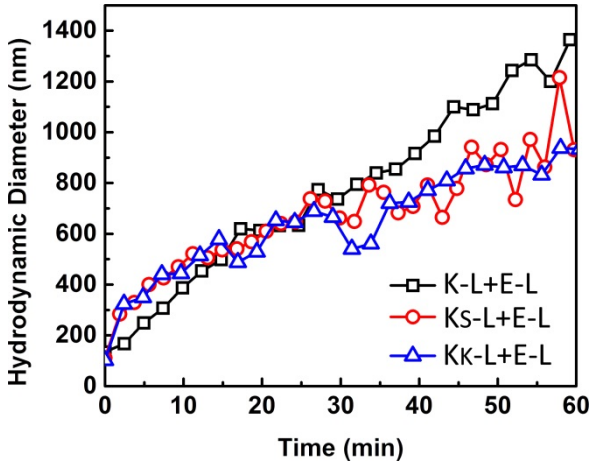

Figure 6. Hydrodynamic diameter increase of the liposomes as a function of time, determined by dynamic light scattering of liposome fusion size increasing. Liposome concentration is 0.1 mM with 1% peptide decoration. See Figure A8 for size increase in the control samples. All the measurements were performed in PBS, pH 7.4, at 25 ^{o}C.

Conclusion

In this study the effect of charge at the f- position of one of the peptides in a heterodimeric coiled coil pair on the rate of liposome fusion was investigated. Studies with the acetylated peptides showed that varying the charge at the 'f' position of coil-K did not alter the ability to form coiled coils. In contrast, when lipidated versions of these peptides were incorporated in liposome membranes, a significant difference in fusion efficiency was observed. Remarkably, the content mixing rate is strongly dependent on mutations of the f-position. By replacing the original negative charge with either no charge or a positively charged side group, the rate of fusion increased as was shown by a content mixing assay. This might be due to lowering the amount of homocoiling in the pre-fusion state resulting in a higher effective peptide concentration. However, more research is needed to confirm this hypothesis.

Experimental section

Materials

Peptides and lipopeptides were synthesized and purified as described previously.[29] DOPE was purchased from Lipoid AG, and cholesterol was obtained from Fluka. DOPE-NBD and DOPE-LR were obtained from Avanti Polar Lipids. All other reagents and solvents were obtained at the highest purity available from Sigma-Aldrich or BioSolve Ltd. and used without further purification. Milli-Q water with a resistance of more than 18.2 MΩ/cm was provided by a Millipore Milli-Q filtering system with filtration through a 0.22 μm Millipak filter.

Liposome Preparation

Liposome for lipid mixing and DLS measurement

Liposomes were composed of DOPC/DOPE/CH (50:25:25 mol%). Fluorescent labeled liposomes also contained 0.5 mol% LR-DOPE and NBD-DOPE. Lipid stock solutions (1 mM) were prepared in chloroform. Lipopeptide stock solutions (10 μM) were prepared in 1:1 (v/v) chloroform:methanol. Liposomes were prepared by drying appropriate volumes of the lipid and lipopeptide stock solutions in a 20 mL bottle under reduced pressure, addition of PBS buffer (pH 7.4) and sonication for ~5 minutes in a bath sonicator with the water bath at 55°C. liposome samples for DLS measurement follow the same procedure as above, but without fluorescent dyes.

Liposome for content mixing

For this assay, 1 mM 1mol % Coil-E decorated liposome was prepared, encapsulating 20 mM sulforhodamine B in pH=7.4 PBS buffer (shortname E-L_{RD}). E-L_{RD} was futher purified by sephadex G-100 column manually (column length= 400 mm, diameter= 30 mm, flow rate= 1 drop s^{-1}), yielding 0.1 mM with 1 mol% Coil-E decoration E_{RD}-L. Meanwhile, 0.1 mM 1 mol % Coil-K decorated liposome was prepared as the way mentioned above (shortname K-L).

Experimental Methods

Experimental diffusion coefficients, D, were measured at 25 °C by dynamic light scattering using a Malvern Zetasizer Nano ZS ZEN3500 equipped with a peltier-controlled thermostatic cell holder. The laser wavelength was 633 nm and the scattering angle was 173˚. The Stokes-Einstein relationship $D = k_BT/3\pi\eta D_h$ was used to estimate the hydrodynamic radius, D_h. Here k_B is the Boltzman constant, and η is the solvent viscosity. The results are expressed as the hydrodynamic diameter with units of nm. For individual liposome batches the sample was allowed to equilibrate for 2 minutes. For DLS time series the solutions were mixed in the cuvette (1000 rpm for 30 seconds). Measurements were started immediately after mixing.

FRET-based lipid mixing experiments were conducted on a Tecan X fluorometer using a 96 well plate. The z-position was 12500 µm, and the gain was optimized according to the amount of fluorophore in the sample. Excitation and emission slits were set at 10 nm. The excitation wavelength was 460 nm, and NBD emission was monitored 535 nm. The measurements were done in room temperature. 100 µL of fluorescent and non-fluorescent liposomes were combined, and for consistent mixing the plate was shaken inside the fluorometer for 30 seconds (2mm linearly, 70 x per minute). Data was collected every 20 seconds for at least 1 hour. Using 0.5 mol% of each fluorophore in the fluorescent liposomes and mixing fluorescent and non-fluorescent liposomes in a 1:1 molar ratio the increase in NBD fluorescence is proportional to lipid mixing. The data was calibrated to show the percentage of liposomes that have undergone lipid mixing by LM (%) = $(I_t - I_0)/(I_{100}-I_0)$ x 100, where I_0 is the NBD intensity of 1:1 (v/v) fluorescent liposomes:PBS, and I_{100} is the NBD intensity of liposomes of the same concentration prepared using an equimolar mixture of fluorescent and non-fluorescent stock solutions. I_0 and I_{100} were monitored with time as they are temperature sensitive. This assay only detects fusion between the original liposomes. e.g. if two pre-fused liposomes fuse the distance between the fluorophores does not change so the event is not detected.

For content mixing assay, the fluorescence signal of the sulforhodamine (λem= 580 nm) was detected once upon 1:1 mixing E_{RD}-L (100ul) with K-L (100 ul). The increase of sulforhodamine B fluorescence is due to a relief of self-quenching following by content mixing, named Ft. The F0 is 100 uL ERD-L with 100 ul PBS, and the F100 is the fluorescence signal intensity after addition of 1% (w/v) Triton X-100 in PBS into the E_{RD}-

L+K-L well. And the content mixing is calculated by CM (%) = $(F_t - F_0)/(F_{100}-I_0)$ x 100. All the data are calculated from 3 times measurements.

For either lipid mixing or content mixing, the standard deviations (σ) are calculated by formula: $\sigma = \sqrt{\frac{1}{N}\sum_{i=1}^{N}(x_i - \mu)^2}$, where $\mu = \frac{1}{N}\sum_{i=1}^{N} x_i$ (x_i is the fluorescence intensity from measurement, N is the number of measurement. In this study, N=3).

Circular dichroism spectra were obtained using a Jasco J-815 spectropolarimeter equipped with a peltier-controlled thermostatic cell holder (Jasco PTC-423S). Spectra were recorded from 260 nm to 200 nm in a quartz cuvette with 5.0 mm pathlength at 25 °C. Data were collected at 1.0 nm intervals with a 1 nm bandwidth and 1 s readings. Each spectrum was the average of 5 scans. The spectra had a baseline of plain liposomes in TES buffer subtracted. The ellipticity is given as the mean residue molar ellipticity, [θ] (10^3 deg cm^2 $dmol^{-1}$), calculated from $[\theta] = (\theta_{obs} \times MRW)/(10 \times l \times c)$, where θ_{obs} is the observed ellipticity in millidegres, MRW is the mean residue molecular weight (i.e. the molecular weight of the peptide divided by the number of amino acid residues), l is the path length of the cuvette in cm and c is the peptide concentration in mg mL^{-1}.

A 1.0 mm quartz cuvette and a final concentration of 200 μM peptide in PBS (pH=7.4). Spectra were recorded from 250 nm to 200 nm at 25 °C. Unless stated otherwise data points were collected with a 0.5 nm interval with a 1 nm bandwidth and scan speed of 1nm per second. Each spectrum was an average of 5 scans. For analysis each spectrum had the appropriate background spectrum (buffer or 50% TFE) subtracted.

For determination of the coiled coil thermal dissociation constant, temperature dependent CD spectra were obtained using an external temperature sensor immersed in the sample.[30, 31] The temperature was controlled with the internal sensor and measured with the external sensor. A 10 mm quartz cuvette was used, and the solutions were stirred at 900 rpm. Spectra were recorded from 250 nm to 200 nm, with data collected at 0.5 nm intervals with a 1 nm bandwidth and a scan speed of 1nm per second. The temperature range was 6 °C to 96 °C with a temperature gradient of 2.0 °C/minute and a 60 s delay after reaching the set temperature. The spectrum of PBS at 6 °C (average of 5 scans) was subtracted from each spectrum. All the thermal unfolding curves were analyzed using a two-state conformation transition model.[32, 33]

The data were analyzed using a two-state unfolding model to determine the fraction folded using Eqn. (2),

$$F_f = ([\theta] - [\theta]_U)/([\theta]_F - [\theta]_U) \quad (2)$$

Where $[\theta]$ is the observed molar ellipticity, $[\theta]_U$ is the ellipticity at 222 nm of the denatured state, as determined from the plateau of the ellipticity vs. temperature curve, and $[\theta]_F$ is the ellipticity at 222 nm of the folded state at that temperature as determined from a linear fit of the initial stages of the ellipticity vs. temperature curve.

The fraction unfolded, F_U, was calculated by Eqn. (3),

$$F_U = 1 - F_f \quad (3)$$

The dimer dissociation constant in the transition zone was calculated using Eqn. (4),

$$K_U = 2P_t F_U^2/F_f \quad (4)$$

P_t is the total peptide concentration. By taking the derivative of the $\ln(K_U)$ vs. temperature and using this in the van't Hoff equation, Eqn. (5), the change in enthalpy associated with unfolding with temperature can be plotted:

$$\Delta H_U = RT^2 \times \frac{d\ln(K_U)}{dT} \quad (5)$$

The gradient of enthalpy vs. temperature plot ΔC_p, is the difference in heat capacity between the folded and unfolded forms, and can be used in the Gibbs-Helmholtz equation adapted to monomer-dimer equilibrium, Eqn. (6), to obtain the Gibbs free energy of unfolding as a function of temperature by least-squares fitting,

$$\Delta G_U = \Delta H_m(1 - T/T_m) + \Delta C_p[T - T_m - T\ln(T/T_m)] - RT\ln[P_t] \quad (6)$$

T_m and H_m are the temperature and enthalpy at the midpoint of the transition at which the fraction of monomeric peptide is 0.5.[12]

Appendix

1. Liquid chromatography mass spectroscopy

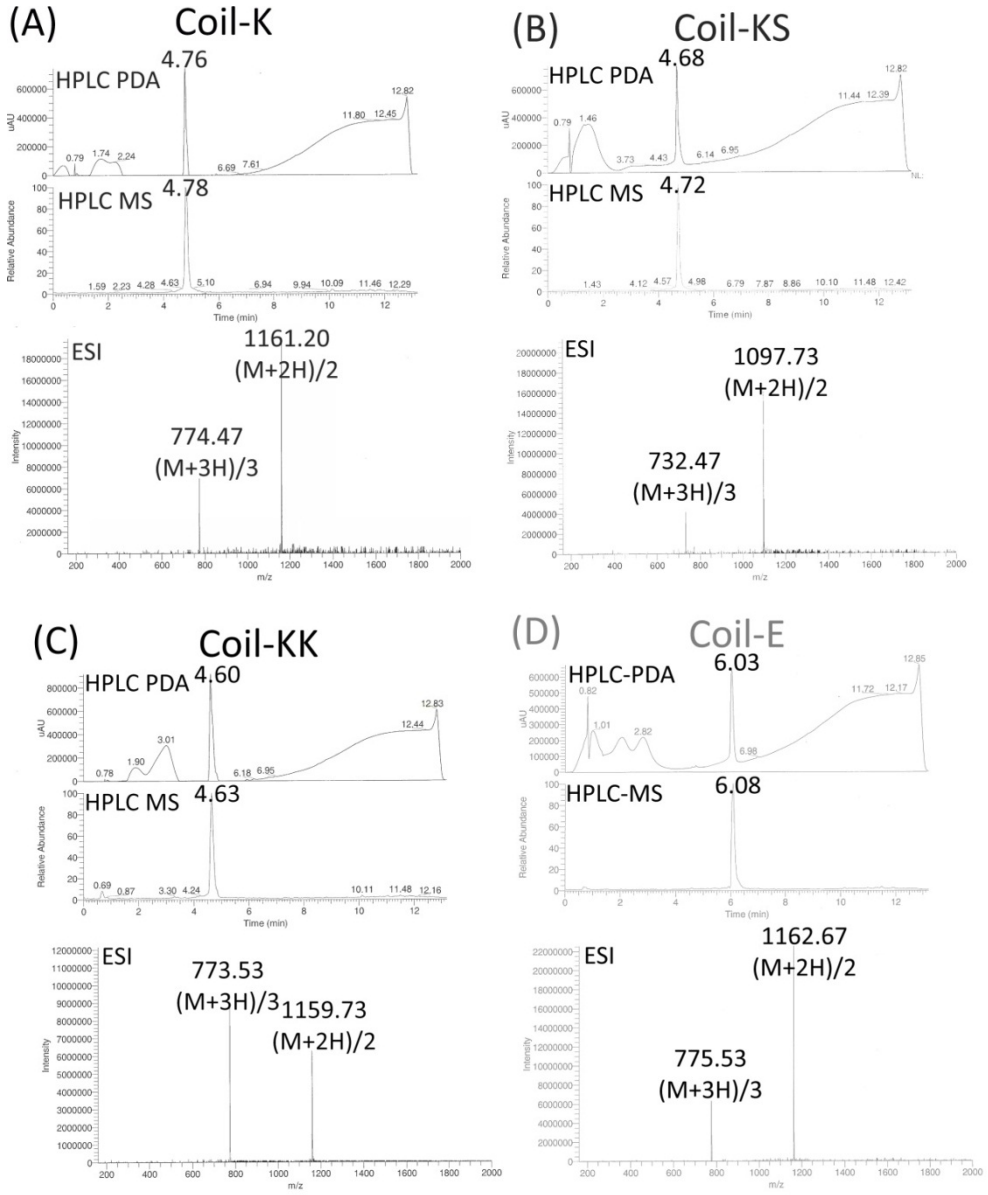

Figure A1. LC-MS spectra of peptide (A) Coil-K, (B) Coil-K_S, (C) Coil-K_K, (D) Coil-E. From top to bottom: UV (ultraviolet-visible) detection wavelength at 214 nm, and ESI (electrospray ionization) mass spectrum.

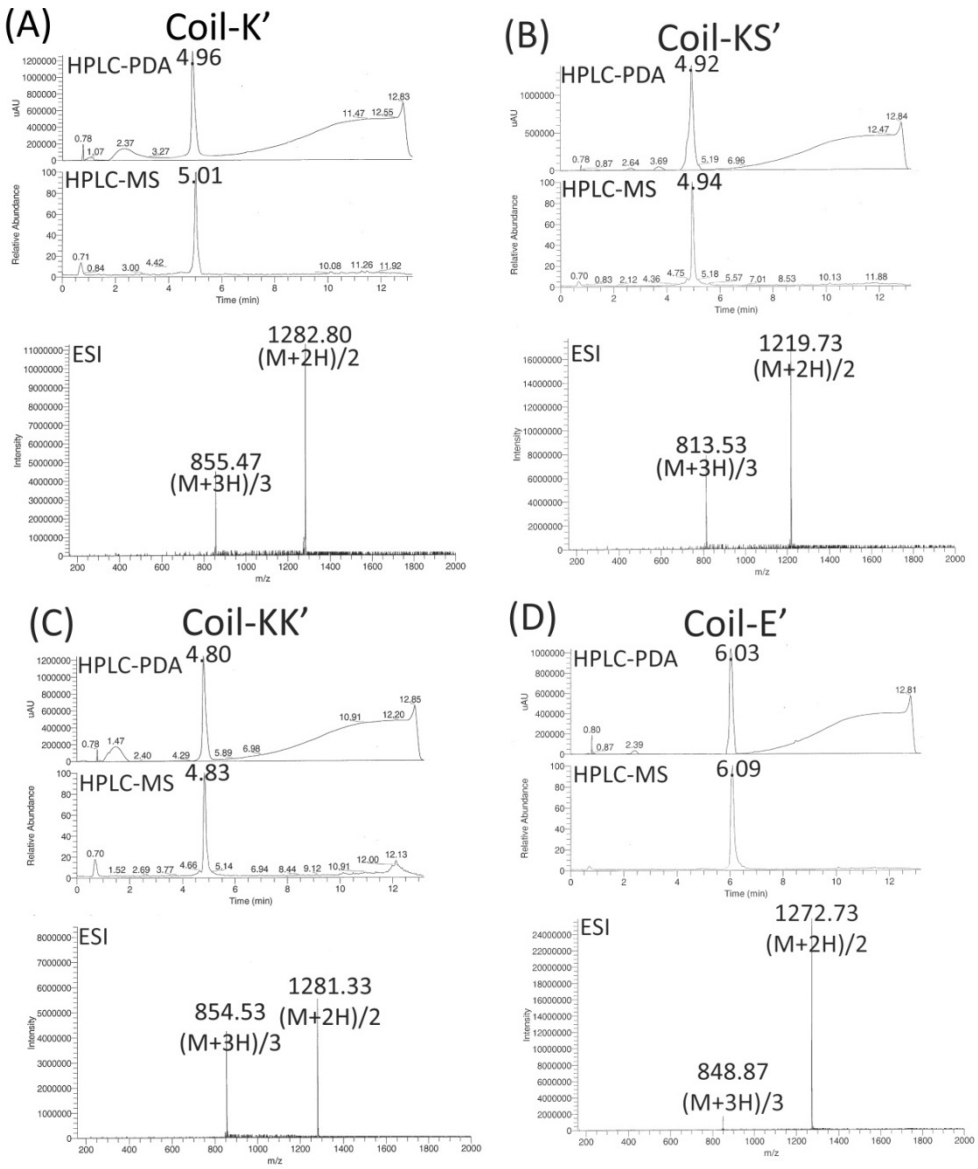

Figure A2. LC-MS spectra of fluorescent labeled peptide (A) Coil-K' (Ac-$(KIAALKE)_3$-GW-$CONH_2$) , (B) Coil-K_S' (Ac-$(KIAALKS)_3$-GW-$CONH_2$), (C) Coil-K_K' (Ac-$(KIAALKK)_3$-GW-$CONH_2$), (D) Coil-E' (Ac-$(EIAALEK)_3$-GW-$CONH_2$). From top to bottom: UV (ultraviolet-visible) detection wavelength at 214 nm, and ESI (electrospray ionization) mass spectrum.

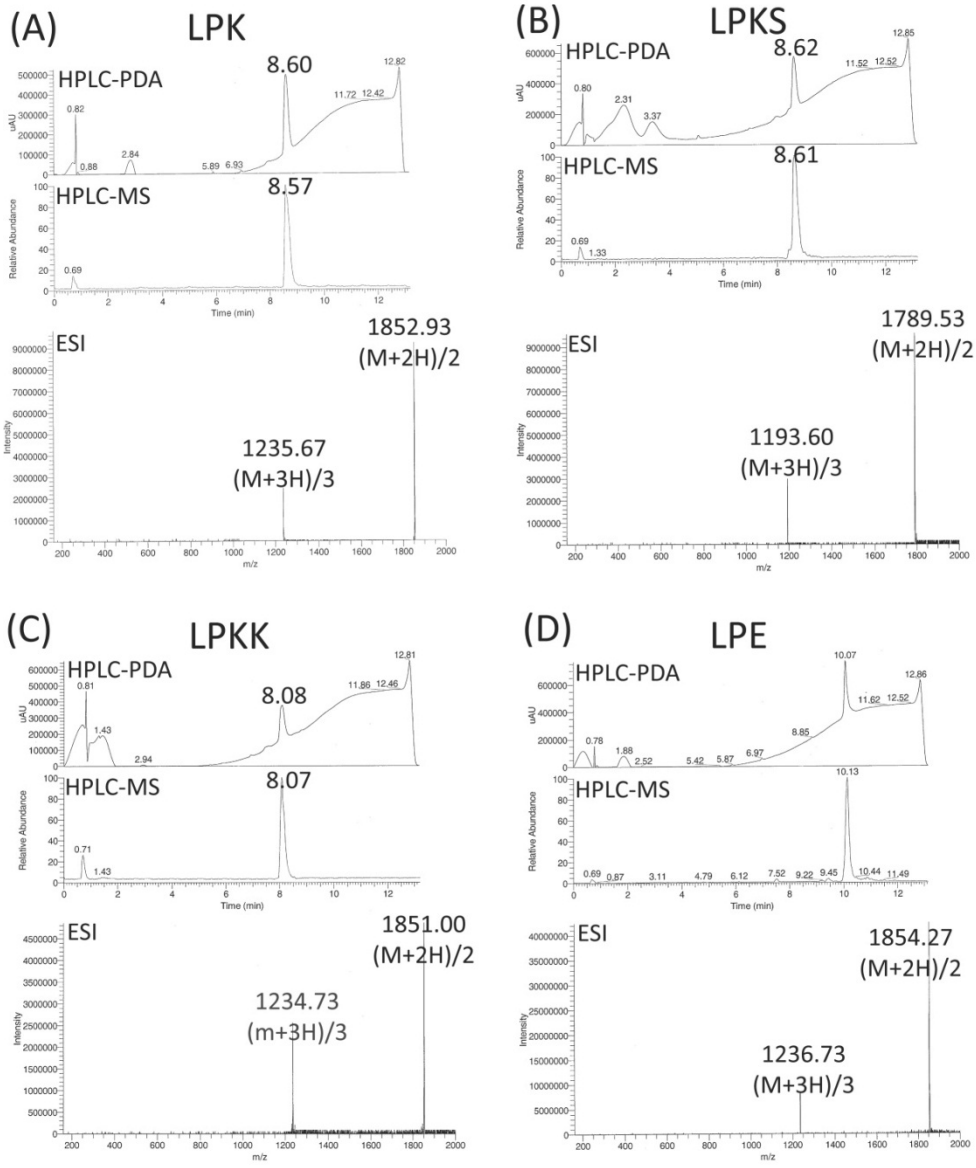

Figure A3. LC-MS spectra of fluorescent labeled peptide (A) LPK, (B) LPK_S, (C) LPK_K, (D) LPE. From top to bottom: UV (ultraviolet-visible) detection wavelength at 214 nm, and ESI (electrospray ionization) mass spectrum.

2. Hyperchem simulation

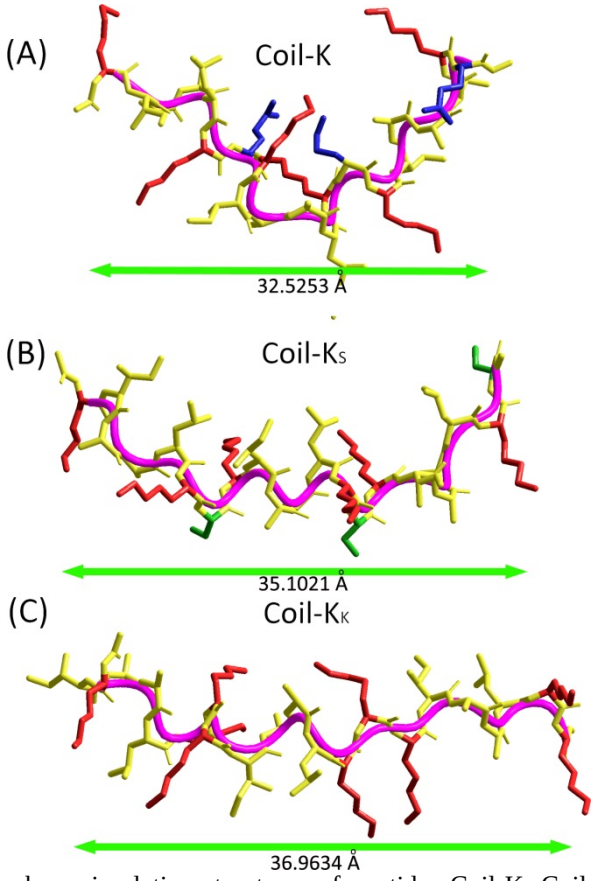

Figure A4. Hyperchem simulation structures of peptides Coil-K, Coil-KS and Coil-KK. The detail simulation method is the same as description in Chapter 3. Green bar indicates peptide length.

3. CD thermal dynamic curves

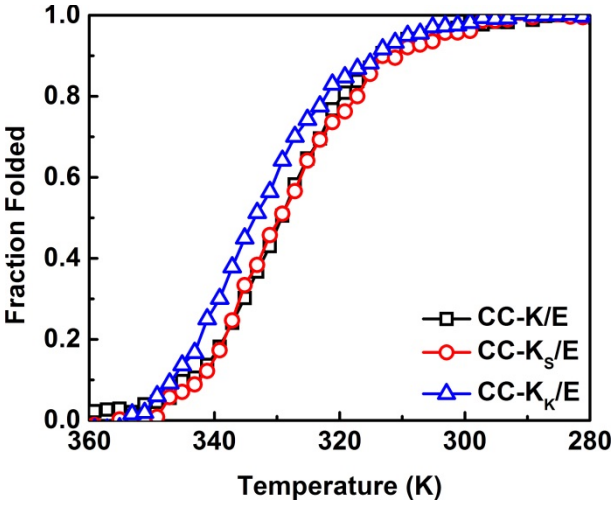

Figure A5. Thermal folding curve based on changes in [θ]222 as followed by CD by decreasing the temperature from 360 to 280 K. [Total peptide]= 40 uM, PBS pH=7.4, 25 ^{o}C, 1 cm quartz cuvette.

4. Liposome fusion control data

4.1 Lipid mixing control

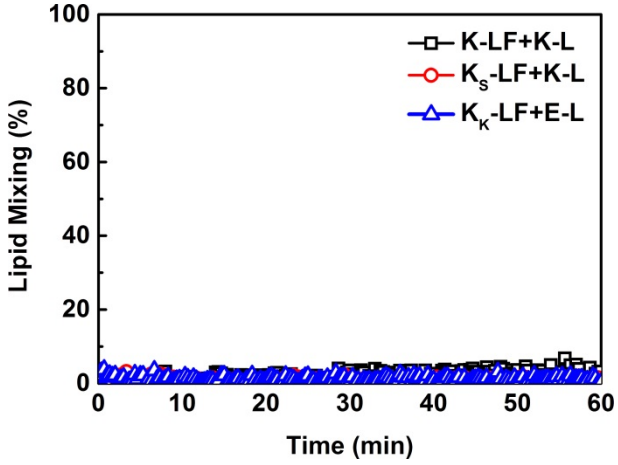

Figure A6. Lipid mixing control as monitored by fluorescence spectroscopy between fluorescent labeled K-LF (and its derivatives) and non-fluorescent K-L (and its derivatives). Fusogen proportion= 1 mol%, [lipids]=0.1 mM, PBS buffer, pH=7.4, 25 ^{o}C.

4.2 Content mixing control

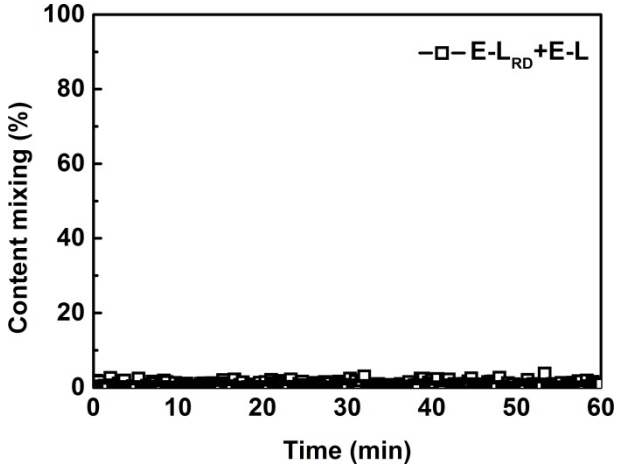

Figure A7. Content mixing control as monitored by fluorescence spectroscopy between sulphorhodamine B loaded E-LRD and non-loaded E-L. Fusogen proportion =1 mol%, [lipids]=0.1 mM, PBS buffer, pH=7.4, 25 ^{o}C.

4.3 DLS size increasing control

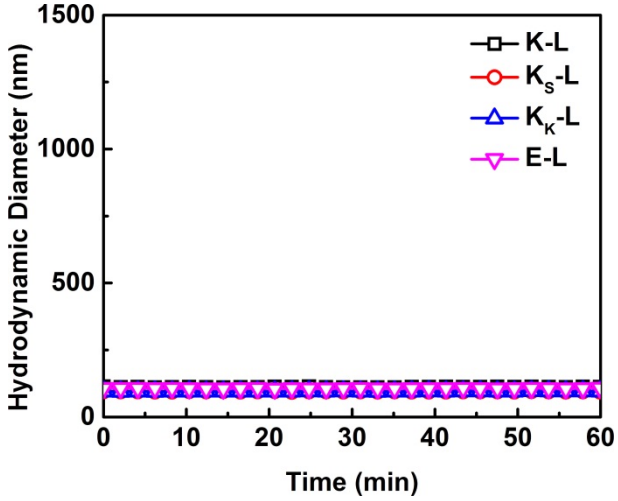

Figure A8. DLS size increasing control as monitored by dynamic light scattering. Fusogen proportion =1 mol%, [lipids]=0.1 mM, PBS buffer, pH=7.4, 25 ^{o}C.

Reference

1. I. Mellman and S. D. Emr, *Journal of Cell Biology*, 2013, **203**, 559-561.
2. T. C. Sudhof and J. E. Rothman, *Science*, 2009, **323**, 474-477.
3. W. Wickner and R. Schekman, *Nature Structural & Molecular Biology*, 2008, **15**, 658-664.
4. W. Antonin, D. Fasshauer, S. Becker, R. Jahn and T. R. Schneider, *Nature Structural Biology*, 2002, **9**, 107-111.
5. H. R. Marsden, I. Tomatsu and A. Kros, *Chemical Society Reviews*, 2011, **40**, 1572-1585.
6. R. Jahn, T. Lang and T. C. Sudhof, *Cell*, 2003, **112**, 519-533.
7. R. Blumenthal, M. J. Clague, S. R. Durell and R. M. Epand, *Chemical Reviews*, 2003, **103**, 53-69.
8. L. V. Chernomordik and M. M. Kozlov, *Nature Structural & Molecular Biology*, 2008, **15**, 675-683.
9. X. C. Chen, D. Arac, T. M. Wang, C. J. Gilpin, J. Zimmerberg and J. Rizo, *Biophysical Journal*, 2006, **90**, 2062-2074.
10. H. R. Marsden, N. A. Elbers, P. H. H. Bomans, N. Sommerdijk and A. Kros, *Angewandte Chemie-International Edition*, 2009, **48**, 2330-2333.
11. H. R. Marsden, A. V. Korobko, T. T. Zheng, J. Voskuhl and A. Kros, *Biomaterials Science*, 2013, **1**, 1046-1054.
12. T. Zheng, J. Voskuhl, F. Versluis, H. R. Zope, I. Tomatsu, H. R. Marsden and A. Kros, *Chemical Communications*, 2013, **49**, 3649-3651.
13. J. R. Litowski and R. S. Hodges, *Journal of Peptide Research*, 2001, **58**, 477-492.
14. P. C. Lyu, M. I. Liff, L. A. Marky and N. R. Kallenbach, *Science*, 1990, **250**, 669-673.
15. H. R. Marsden, T. T. Zheng and A. Kros, *Abstracts of Papers of the American Chemical Society*, 2013, **245**.
16. C. N. Pace and J. M. Scholtz, *Biophysical Journal*, 1998, **75**, 422-427.
17. B. Apostolovic and H. A. Klok, *Biomacromolecules*, 2008, **9**, 3173-3180.
18. Y. H. Chen, J. T. Yang and K. H. Chau, *Biochemistry*, 1974, **13**, 3350-3359.
19. C. Y. Huang, *Methods in Enzymology*, 1982, **87**, 509-525.
20. Z. D. Hill and P. Maccarthy, *Journal of Chemical Education*, 1986, **63**, 162-167.
21. J. A. Boice, G. R. Dieckmann, W. F. DeGrado and R. Fairman, *Biochemistry*, 1996, **35**, 14480-14485.
22. J. R. Litowski and R. S. Hodges, *Journal of Biological Chemistry*, 2002, **277**, 37272-37279.
23. J. Eisinger, B. Feuer and A. A. Lamola, *Biochemistry*, 1969, **8**, 3908-&.
24. K. Park, A. Perczel and G. D. Fasman, *Protein Science*, 1992, **1**, 1032-1049.
25. M. Cascio and B. A. Wallace, *PROTEIN PEPT.LETT.*, 1994, **1**, 136-140.
26. B. A. Wallace, J. G. Lees, A. J. W. Orry, A. Lobley and R. W. Janes, *Protein Science*, 2003, **12**, 875-884.
27. N. E. Zhou, C. M. Kay and R. S. Hodges, *Biochemistry*, 1992, **31**, 5739-5746.

28. I. Tomatsu, H. R. Marsden, M. Rabe, F. Versluis, T. Zheng, H. Zope and A. Kros, *Journal of Materials Chemistry*, 2011, **21**, 18927-18933.

29. H. Robson Marsden, N. A. Elbers, P. H. H. Bomans, N. A. J. M. Sommerdijk and A. Kros, *Angewandte Chemie International Edition*, 2009, **48**, 2330-2333.

30. S. M. Kelly and N. C. Price, *Biochimica Et Biophysica Acta-Protein Structure and Molecular Enzymology*, 1997, **1338**, 161-185.

31. S. M. Kelly, T. J. Jess and N. C. Price, *Biochimica Et Biophysica Acta-Proteins and Proteomics*, 2005, **1751**, 119-139.

32. P. Lavigne, M. P. Crump, S. M. Gagne, R. S. Hodges, C. M. Kay and B. D. Sykes, *Journal of Molecular Biology*, 1998, **281**, 165-181.

33. P. Lavigne, L. H. Kondejewski, M. E. Houston, F. D. Sonnichsen, B. Lix, B. D. Sykes, R. S. Hodges and C. M. Kay, *Journal of Molecular Biology*, 1995, **254**, 505-520.